Polymorphism in Halogen-Ethane Derivatives: CCl3-CCl3 and ClF2C-CF2Cl

Philippe Négrier, Josep Ll Tamarit, María Barrio, Denise Mondieig

Polymorphism in Halogen-Ethane Derivatives: CCl_3-CCl_3 and ClF_2C-CF_2Cl

Philippe Negrier,[†] Josep Ll. Tamarit,*[,‡] María Barrio,[‡] and Denise Mondieig[†]

[†]Université de Bordeaux, LOMA, UMR 5798, F 33400 Talence, France CNRS, LOMA, UMR 5798, F 33400 Talence, France

[‡]Grup de Caracterització de Materials, Department de Física i Enginyeria Nuclear, ETSEIB, Diagonal 647, Universitat Politècnica de Catalunya, 08028 Barcelona, Catalonia, Spain

ABSTRACT: The polymorphism of hexachloroethane, Cl_3C-CCl_3, has been reinvestigated by means of X ray and neutron scattering. The long time unknown structure of the intermediate phase II of Cl_3C-CCl_3 has been determined as monoclinic $C2/m$, with lattice parameters a = 17.9835(21) Å, b = 10.3642(11) Å, c = 6.3014(8) Å, and β = 94.410(5)° at 323 K, Z = 6. The polymorphism of 1,2 dichloro 1,1,2,2 tetrafluoro ethane, ClF_2C-CF_2Cl, has also been investigated, and the structure of the intermediate phase II has been found to be orthorhombic ($Cmca$, Z = 4) with lattice parameters a = 6.305(4) Å, b = 10.177(12) Å, c = 8.714 (7) Å. The high temperature phase I of ClF_2C-CF_2Cl has been found to be isomorphous with the orientationally disordered phase I of Cl_3C-CCl_3 (body centered cubic, $Im3m$), a consequence of the pseudospherical molecular shape of halogeno ethane $C_2X_{6-n}Y_n$ (X = Cl, Y = F) molecular crystals. The similarities of the intricate disorder of the intermediate phases II of both Cl_3C-CCl_3 and ClF_2C-CF_2Cl compounds are analyzed, together with the influence of the conformational disorder appearing in the last compound.

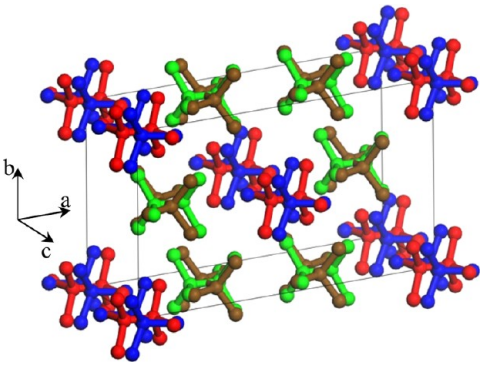

1. INTRODUCTION

While thermodynamic and heat transfer properties of some hydrochlorofluorocarbons have been investigated due to the industrial use for refrigeration systems in order to replace the chlorofluorocarbons,[1,2] low temperature crystallographic information was scarce or even nonexistent due to the difficulties of growing single crystals at low temperature. It should be mentioned the noticeable work developed by Brunelli and Fitch[3,4] for several of these compounds by means of condensation of the vapor phase and structural determination through synchrotron radiation. The low temperature monoclinic ordered structures as well as the high temperature bcc lattice of 1,1,1,2,2 pentafluoroethane (F_3C-CF_2H) and 1,2 difluoroethane ($H_2FC-CFH_2$)[3] and the disordered hexagonal structures of 1,2 dichlorotrifluoroethane ($ClF_2C-CFHCl$) and 2 chloro 1,1,1,2 tetrafluoroethane ($ClFHC-CF_3$)[4] were determined in that way.

Pioneer crystallographic studies on single crystals among simplest halogen ethane derivatives were performed on 1,2 diiodoethane (IH_2C-CH_2I) as early as 1935 by Klug.[5,6] Within the hydrochlorocarbons, single crystal studies were later carried on for 1,2 dichloroethane (ClH_2C-CH_2Cl) (monoclinic $P2_1/c$) by Milberg et al.,[7] the monoclinic structure being later confirmed by Boese et al.[8] By increasing the number of chlorine atoms within the halogenoethane derivatives, we must mention here the recent works by Katrusiak et al. Several of these works have shown the extraordinary plentiful and widespread polymorphism on related compounds at normal and high pressure. Thus, the low temperature monoclinic ($C2/c$) phase (at normal pressure) of 1,1,1,2 tetrachloroethane (Cl_3C-CH_2Cl), for which only one conformation exists, has been determined to be disordered.[9] The orientational disorder concerns chlorine and hydrogen atoms with occupancies of 0.7 and 0.3, respectively, with no significant changes as a function of temperature. Similar disorder, but strongly temperature dependent as far as the occupancy factors are concerned, was found in 1,1,2 trichloroethane.[10] Even the simple 1,2 dichloroethane (ClH_2C-CH_2Cl) compound displays common sites for the chlorine atoms, whereas carbon and hydrogen atoms are disordered.[8,11] The compound 1,1,2,2 tetrachloroethane ($Cl_2HC-CHCl_2$) exhibits the so called conformational polymorphism, because the *gauche* conformers control the low temperature normal pressure orthorhombic phase, whereas the *trans* conformers govern the denser high pressure monoclinic polymorph.[12] The difference between polymorphs is intrinsically linked to the intermolecular interactions (mainly due to Cl···Cl contacts) because the energy difference between conformers is virtually zero, and thus the higher molecular symmetry of the *trans* conformers favors a better packing.

In some cases the molecules do not exhibit conformational disorder, but disordered structures have also been found.[13]

In addition to this wealth of possible different packing and interactions, we must add the fact that for almost all of halogen ethane

Table 1. Temperature Transitions T_c and Enthalpy ΔH Changes, Slope of the Temperature Pressure Two Phase Equilibria dT_c/dp, and Volume Changes Δv for the Phase Transitions of Cl_3C-CCl_3 and ClF_2C-CF_2Cl

compound	phase change	T_c K	ΔH kJ mol^{-1}	$(dT_c/dp)^E$ K MPa^{-1}	$(dT_c/dp)^{CC}$ K MPa^{-1}	Δv cm^3 mol^{-1}	ref
Cl_3C Cl_3	III II	318.2			0.296 ± 0.047[a]	2.39 ± 0.25	this work
		318.2	2.565		0.285	2.30	23
				0.287[b]			29
ClF_2C CF_2Cl		109.3 ± 0.2	1.212 ± 0.013				37
Cl_3C Cl_3	II I	343.9			0.303 ± 0.026[a]	7.24 ± 0.23	this work
		344.6	8.222		0.278	6.63	23
				0.340[b]			29
ClF_2C CF_2Cl		134.6 ± 0.1	2.628 ± 0.003				37
Cl_3C Cl_3	I L	458	9.749				23
ClF_2C CF_2Cl		180.62 ± 0.02	1.510 ± 0.003				37

[a]Enthalpy changes from adiabatic calorimetry[23] were used. [b]Calculated from fits of the experimental values published by Knorr.[29]

derivatives, due to their pseudospherical molecular symmetry, an orientationally disordered (OD) high temperature phase is expected.[14] Actually, this high molecular symmetry enables reorientation of molecules without a noticeable change of molecular volume, one of the well known conditions to the existence of an OD or plastic phase.[15,16] It is quite obvious that intramolecular rotations around the C−C molecular axis give rise to energetically equivalent or unequivalent conformations, the latter with a small energy difference, for which the lattice symmetry must "accommodate" providing the polymorphic behavior.

Within the context of these results, some authors considered that molecular conformation is the key factor in the structure (and thus in the polymorphic behavior) of flexible molecules, even for those as simple as halogen ethane series.[17,18] Nevertheless we must point out that even with the great power of molecular simulations we are still far away for predicting polymorphs, a topic to which great efforts are spent at present.[19] A telling example is the Cl_3C-CCl_3 compound: it can be classified as one of the "simplest" halogenated derivatives due to its high molecular symmetry and because it is devoid of conformations. Curiously, despite of the great number of studies by using different kinds of techniques which enabled researchers to describe the polymorphic behavior, structural details of the intermediate solid phase (phase II) are still unknown.

Some examples in which only one conformation is present have been recently published.[13] They concern the cases of CF_3-CF_2Cl and CCl_3-CF_2Cl. The former displays, in addition to the high temperature OD phase, a low temperature fully ordered monoclinic ($P2_1/n$) structure. The latter, on the contrary, displays a low temperature phase with site occupancy disorder between one F and one Cl atom. It then means that in spite of the close molecular similarity, fine tuning interactions give rise to different polymorphisms, reinforcing the difficulty to predict polymorphism in organic compounds.

The present experimental work was undertaken to complete the crystal structure of phase II and to reexamine the phase transitions of hexachloroethane (Cl_3C-CCl_3) at normal pressure (i.e., in equilibrium with the vapor pressure). Because previous attempts using single crystal methods were not successful,[20] X ray and neutron powder diffraction were used. We will demonstrate that the claimed complexity of the structure of phase II concerns both the special number of molecules in the unit cell as well as the disorder of the motifs building the unit cell. For such an avail, the polymorphism of Cl_3C-CCl_3 has been revisited and the long time unknown structure of the intermediate phase II has been determined to be monoclinic with space group $C2/m$. At normal pressure, Cl_3C-CCl_3 crystallizes on cooling at ca. 458 K into an OD body centered cubic (bcc) phase I, the disorder of which being studied for many different experimental techniques as well as by using molecular dynamics simulations.[20−36] Upon further cooling, it transforms at about 345 K to phase II, the symmetry of which is unknown, but for which some disorder is still present. This phase is stable at normal pressure till 318 K, where it transforms to a low temperature fully ordered orthorhombic phase.[21,33]

ClF_2C-CF_2Cl (1,2 dichloro 1,1,2,2 tetrafluoro ethane) molecule has two rotational isomers, *trans* and *gauche* (dihedral angles 180° and 62.5°, respectively).[37−39] The dipolar form, *gauche*, displays a dipole moment of 0.81 D, whereas the *trans* form is devoid of dipole. Both isomers are known to exist in the gas, liquid state and in solid forms I and II, whereas in the solid form III only the *trans* isomer is present.[24,38] Transition temperatures and enthalpy changes determined by adiabatic calorimetry are gathered in Table 1. It should be noticed that the vaporization process for this compound at normal pressure (277 K) is below room temperature, whereas Cl_3C-CCl_3 does not exhibit a measurable temperature domain for the liquid state because vaporization follows the melting at normal pressure.[40,41]

For both compounds the enthalpy change from III to II is smaller than that from II to I, an experimental fact quite common for materials exhibiting plastic phases with additional solid−solid phase transitions at low temperatures, indicating that on heating the "increase of disorder" is stronger in the transition to the OD phase, whereas lower transitions involved just minor changes.[42]

The structure of phase II of Cl_3C-CCl_3 has been compared to that of phase II of ClF_2C-CF_2Cl, for which also for the first time it has been determined as orthorhombic (*Cmca*). In spite of the differences in the space groups of both phases, we will show that the main features concerning disorder are shared.

2. EXPERIMENTAL SECTION

Cl_3C-CCl_3 compound was purchased from Aldrich with a chemical purity of 99%, while ClF_2C-CF_2Cl was purchased from ABCR with purity of 99%.

The gas sample ClF_2C-CF_2Cl was transferred from the supplier container to the neutron diffraction cell by means of a specially designed system for hydrogen condensation at the Institute Laue Langevin (ILL) which enables the control of the pressure. The diffraction cell was placed into an Orange cryostat the temperature of which was continuously monitored.

As for Cl_3C-CCl_3, the powder was gently crushed before being introduced into the neutron diffraction cell or into 0.2 mm diameter Lindemann capillaries for the X ray measurements.

2.1. Neutron Powder Diffraction Measurements. Neutron powder diffraction patterns of C_2Cl_6 were collected at 10 and 150 K by means of the high resolution powder diffractometer SPODI at FMRII (Technische Universität Darmstadt, Germany) within the standard configuration ($2\theta_{max}$ = 155°) and λ = 2.537 Å.[43] Low temperature neutron measurements were envisaged in order to investigate the existence of new phases in that domain. Patterns at 330 and 400 K were also recorded, but some temperature instabilities of the cryostat made them unsuitable for crystal structure resolution. Thus, the structure of the intermediate phase II of Cl_3C-CCl_3 was studied only by X ray diffraction experiments.

Patterns of the condensed ClF_2C-CF_2Cl compound were collected at 10, 120, and 155 K using the high resolution D2B instrument at ILL (Grenoble, France).[44] High resolution data from the equatorial detector bank were obtained by using a wavelength of λ = 2.398 Å in a 2θ range from 20° to 160° with a step size of 0.05°. Because of the aforementioned problems concerning the incomplete II to III transformation, the pattern at 10 K could not be indexed, and thus the structure of phase III remains unknown. Even the collected pattern at 120 K (phase II) showed three Bragg peaks of the high temperature cubic phase I. Nevertheless, because of the high symmetry of phase I the pattern collected at 120 K was indexed once the 2 theta regions containing the Bragg peaks of phase I were excluded.

2.2. X-ray Powder Diffraction Measurements. X ray powder patterns were isothermically recorded by means of a horizontally mounted INEL cylindrical position sensitive detector (CPS120). The detector, used in Debye−Scherrer geometry (transmission mode), consists of 4096 channels and enables a simultaneous recording of the diffraction profile over a 2θ range between 2 and 115° (angular step of 0.029° in 2θ). Monochromatic Cu $K_{\alpha 1}$(λ = 1.5406 Å) radiation was selected by means of an asymmetric focusing incident beam curved quartz monochromator. The generator power was set to 1.0 kW (40 kV and 25 mA). External calibration was performed by using $Na_2Ca_2Al_2F_{14}$ mixed with silver behenate.[45,46]

The temperature was controlled by means of a liquid nitrogen 600 series Cryostream Cooler from Oxford Cryosystems with a temperature accuracy of 0.1 K and similar for fluctuations. Measurements were performed from 100 K till 375 K every 30 K up to 280 K and less when approaching the III to II phase transition, and every 5 K for the temperature range of phases II and I.

3. RESULTS AND DATA ANALYSIS

3.1. Structure Determination of the Low-Temperature Phases of Cl_3C-CCl_3. *Phase III.* Neutron and X ray patterns of the low temperature orthorhombic phase III were indexed according to the *Pnma* space group reported by Sasada et al.[34] A Rietveld profile refinement[47] by means of the Materials Studio software[48] was conducted by using the atomic coordinates of the molecule in the asymmetric unit given by Sasada and Atoji[34] as starting parameters (see Figure 1). A glance to Figure 1 shows that in spite of the efforts to correct the preferred orientation of the sample, some Bragg peaks with high intensity give rise to a relative noticeable difference between calculated and experimental patterns.

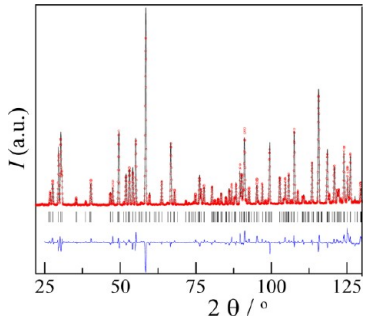

Figure 1. Experimental (red circles) and calculated (black line) neutron diffraction patterns along with the difference profile (blue line) and Bragg reflections (vertical sticks) for the final Rietveld refinement of *Pnma* orthorhombic phase III of CCl_3-CCl_3 (at 10 K).

The parameters refined in the procedure both for neutron and X ray measurements are gathered in Table 2. Gaussian and pseudo Voigt fits for neutron and X ray were used, respectively, for the Bragg peak profiles. The coordinates of the atoms of the asymmetric unit are given as Supporting Information (Table S1) for the measurement at 10 K (neutron diffraction) and in Table S2 for the measurement at 296 K (X ray diffraction). In both cases, taking the advantage of the existence of a unique molecular conformation and an ordered structure, bond distances and angles were finally refined according to the minimization energy process, which converged giving the values reported in the aforementioned tables.

The orthorhombic structure of phase III of Cl_3C-CCl_3 (shown in Figure 2) has been largely discussed after the pioneer work of Hohlwein et al. in 1979.[22] Moreover, a mechanism for the phase transition from phase III to phase I through the intermediate phase II has been proposed from Woost and Bougeard.[21] According to them, it consists, first, on high amplitude motions around an axis perpendicular to the C−C intramolecular axis and parallel to the *b* orthorhombic lattice axis, giving rise to a disorder within the (*a*, *c*) orthorhombic plane in such a way that while the amplitude of the motions increases the angle between *a* and *c* also goes from 90° to the β angle of the monoclinic phase. We should now keep in mind the recent work[13] concerning the structure of the low temperature phase of CCl_3-CF_2Cl, isostructural to the phase III of Cl_3C-CCl_3 (the difference being the site occupancy disorder between one F and one Cl atoms, with equal occupancy factor of 0.5). For such a case, the low temperature phase transforms to the high temperature orientationally disordered phase I (*Im*3*m*) without an intermediated phase as for Cl_3C-CCl_3.

In both CCl_3-CF_2Cl and Cl_3C-CCl_3 cases the C−C bonds lie in the (0*k*0) plane, the molecules being alternatively tilted with respect to the [00*l*] direction by an angle of 7.0° (at 125 K) and 6.7° (at 5 K) in CCl_3-CF_2Cl and 13.2° in C_2Cl_6 (at 10 K).

Phase II. We have built up a rigid body molecule by means of the software Forcite from Materials Studio package together with the Compass forcefield. The minimization energy process converged to an almost perfect tetrahedral molecular symmetry (C−C = 1.586 Å; C−C1 = 1.776 Å; C−C−Cl = 110.48°; Cl−C−Cl = 108.45°). These values are very close to those determined by the final energy minimization of the structure of phase III.

The potential solutions of the cell parameters and space groups were obtained using X Cell software[49] available in the module Powder Indexing of Materials Studio applied to the X ray powder diffraction at 323 K. Cell parameters and space groups compatible with the experimental pattern were refined by means of a Pawley procedure by minimizing the weighted R_{wp} factor. The analysis of the systematic absences for a monoclinic indexing enables us to determine the space group, *C*2/*m*.

In general, such space group *C*2/*m* contains *Z* = 8, but reasonable values of density (which should give compatible volume changes obtained by means of the Clausius−Clapeyron equation, see Table 1) indicate that the number of molecules should be *Z* = 6. For an ordered structure with such a *Z* the selected space group would provide two independent molecules, both on the mirror plane perpendicular to the *b* axis and with the C−C direction and two chlorine atoms on the mirror, thus providing four molecules for the unit lattice for each independent

Table 2. Results from the Rietveld Refinement of the Low Temperature Phase III and the Intermediate Phase II of Cl_3C-CCl_3 and Intermediate Phase II of ClF_2C-CF_2Cl

chemical formula	$Cl_3C\ CCl_3$				$ClF_2C\ CF_2Cl$
M/g mol^{-1}	236.739				170.921
phase		Phase III		Phase II	Phase II
2θ-angular range	25 152°	25 152°	15 90°	9 70°	20 90°
space group, Z	*Pnma*, 4	*Pnma*, 4	*Pnma*, 4	*C*2/*m*, 6	*Cmca*, 4
a /Å	11.1677(5)	11.2853(6)	11.5494(9)	17.9835(21)	6.305(4)
b/Å	9.9851(5)	10.0394(5)	10.1825(7)	10.3642(11)	10.177(12)
c/Å	6.3099(3)	6.3627(4)	6.4002(5)	6.3014(8)	8.714(7)
β/°				94.410(5)	
V/Z/Å^3	175.90	180.22	188.17	195.17	139.77
temperature (K)	10	150	296	323	120
D_x/g cm^{-3}	2.235	2.181	2.089	2.014	2.031
radiation type,	Neutron	Neutron	X-ray	X-ray	Neutron
λ/Å	2.537	2.537	1.5406	1.5406	2.398
2θ-shift (zero correction)	0.1023(12)	0.0950(12)	0.0001(7)	0.0108(11)	0.138(7)
	profile (pseudo-Voigt) parameters				
Na			0.274(18)	0.314(16)	
Nb					
asymmetry parameters				H = 0.0163(4)	
				S = 0.0164(4)	
	reliability parameters				
R_{wp} (%)	12.7	9.82	5.21	3.07	6.91
R_p (%)	8.95	6.92	3.40	2.17	5.10
	peak width parameters				
U	0.0212(13)	0.0296(21)	0.0363(41)	0.022(7)	2.06(32)
V	0.0402(40)	0.045(5)	0.0296(31)	0.007(4)	2.12(30)
W	0.1110(24)	0.1075(25)	0.0126(6)	0.0076(7)	0.68(6)
overall isotropic temperature factor, U/Å^2	0.0000(6)	0.0087(6)	0.0356(10)	0.060(4)	0.006(6)
	preferred orientation[a] (Rietveld-Toraya function)				
a^a	0.9589	0.9713	0.4268	0.7128	0.335(5)
b^a	0.2837	0.2367	0.4437	0.6661	0.487(7)
c^a	0.0000	0.0239	0.7880	0.2196	0.807(3)
G2	0.7856	0.9295	0.1110	0.9860	
G1	0.7365	1.1882	0.0629	1.6484	
R0					0.254(10)

[a]R0: March Dollase parameter.[50] G1, G2: Rietveld Toraya parameters.[51]

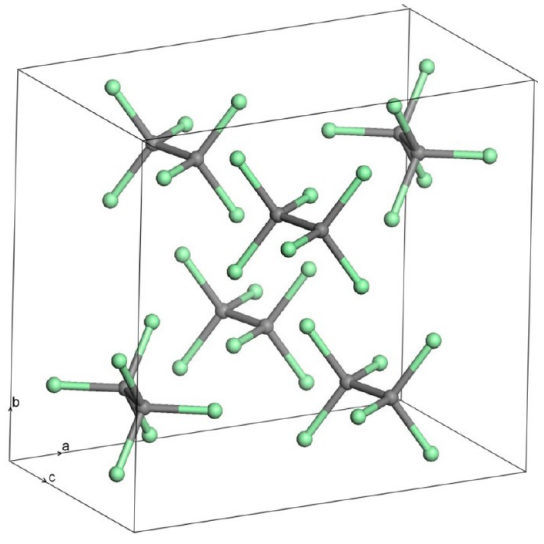

Figure 2. *Pnma* structure of phase III of Cl_3C-CCl_3 obtained from neutron powder diffraction at 10 K (Cl green; C gray).

molecule. But one of the independent molecules is also on the (0,0,0) with the center of the C−C bond lying along the binary axis; this one contributes to only two molecules to the unit cell, while the other gives four molecules in the unit. Thus, it finally would account for the six molecules in the unit cell. Nevertheless, such an exercise did not provide the right solution as noticeable discrepancies between the experimental and calculated pattern emerged.

The final solution here was found when the structure is assumed to be disordered. Thus, there are not two independent molecules but four, with site occupancy factors for them of 0.5 (see Figure 3). Two molecules are at the center (red and blue molecules), providing two molecules to the unit cell (read also [2 + 2]*0.5) and two additional molecules (brown and green) contributing with 2 + 2 molecules to the unit cell (read also [4 + 4]*0.5), accounting then for the final value $Z = 6$. The molecules at the center (0,0,0) (red and blue in Figure 3, and labeled as "1" and "2" in Table 3) cross at the center of the C−C bond (for symmetry reasons), the C−C bonds of both molecules being almost perpendicular (89.4°). The two last molecules (green and brown in Figure 3 labeled as "3" and "4" in Table 3) do not cross at the middle of the C−C bond as the only constraint is the mirror, also being almost perpendicular (80.7°). Molecules "1" (red) and "3" (green) have almost the same orientation, the angle with the z axis being 81.9 ° and 80.7°, whereas the molecules "2" (blue) and "4" (brown) are a little bit tilted (−7.5° and 2.7°). For

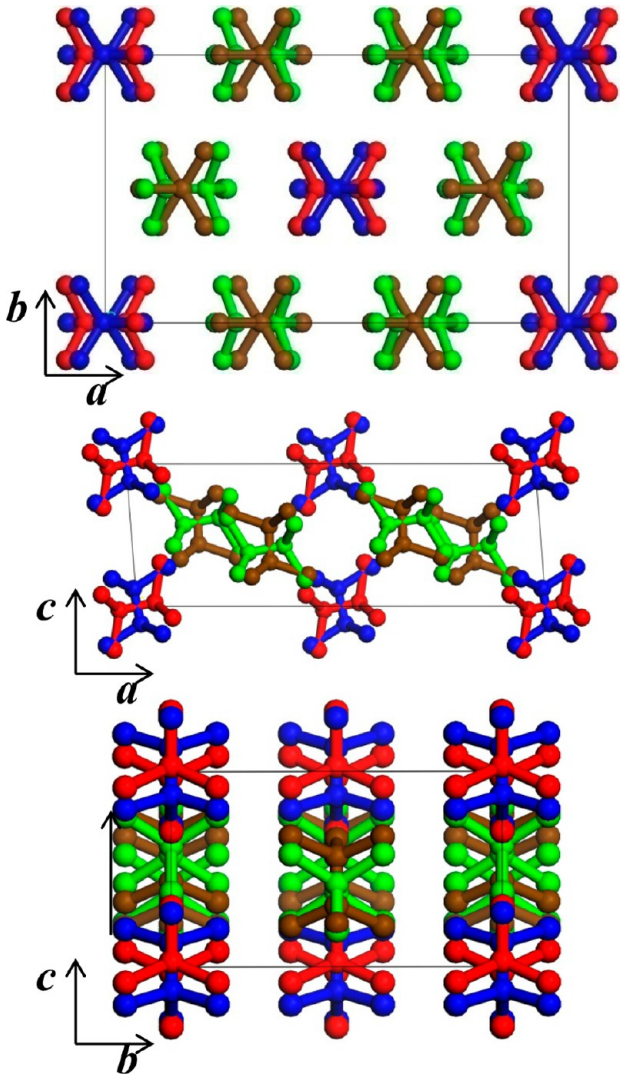

Figure 3. Projection of the *C*2/*m* structure of phase II of Cl_3C-CCl_3 in the (00*l*) (top), (0*k*0) (middle), and (*h*00) (bottom) planes.

Table 3. Fractional Coordinates of the Intermediate Monoclinic Phase II of Cl_3C-CCl_3 Obtained at 323 K by Using X ray Powder Diffraction

molecule	atom	X	Y	Z	occupancy
1	C(1)	0.0058	0.0000	0.124	0.5
	Cl(11)	0.0817	0.0000	0.275	0.5
	Cl(12)	0.0563	0.1390	0.193	0.5
2	C(2)	0.0438	0.0000	0.027	0.5
	Cl(21)	0.0651	0.0000	0.307	0.5
	Cl(22)	0.0846	0.1390	0.081	0.5
3	C(3)	0.3375(27)	0.0000	0.564(5)	0.5
	C(4)	0.3334(27)	0.0000	0.311(5)	0.5
	Cl(31)	0.2464(27)	0.0000	0.654(5)	0.5
	Cl(32)	0.3855(27)	0.1390	0.666(5)	0.5
	Cl(41)	0.4245(27)	0.0000	0.220(5)	0.5
	Cl(42)	0.2854(27)	0.1390	0.208(5)	0.5
4	C(5)	0.2824(25)	0.0000	0.378(9)	0.5
	C(6)	0.3703(25)	0.0000	0.426(8)	0.5
	Cl(51)	0.2373(25)	0.0000	0.619(8)	0.5
	Cl(52)	0.2533(25)	0.1390	0.229(8)	0.5
	Cl(61)	0.4154(25)	0.0000	0.185(8)	0.5
	Cl(62)	0.3993(25)	0.1390	0.575(8)	0.5

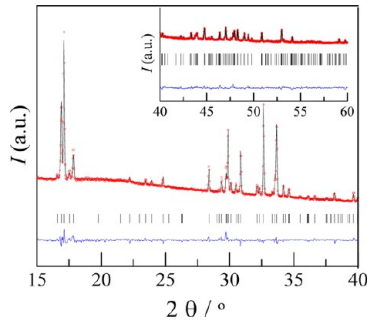

Figure 4. Experimental (red circles) and calculated (black line) diffraction patterns along with the difference profile (blue line) for the final Rietveld refinement of the intermediate phase II of Cl_3C-CCl_3 at 323 K. Inset corresponds to the scale for the data with $2\theta > 40°$.

both sets of molecules it is clearly seen in Figure 3 ((0*k*0) plane) that the Cl−C−C−Cl zigzag is reversed. The different projections of the structure of the intermediate phase II of Cl_3C-CCl_3 are shown in Figure 3.

The experimental and the final calculated profiles are shown in Figure 4 together with the difference plot between them. The parameters refined in the procedure are collected in Table 2, and the coordinates of the atoms of the asymmetric unit are given in Table 3. Because of the disorder we did not undertake a minimization of energy of the structure, so molecular bond length and angles were kept according to the initial molecular minimization.

3.2. Structure Determination of the Low-Temperature Phase II of ClF_2C-CF_2Cl. The neutron powder diffraction pattern recorded on D2b (ILL) at 120 K for phase II of ClF_2C-CF_2Cl was indexed based on the first 16 Bragg peaks using the X Cell software available in the module Powder Indexing of Materials Studio.

The software Forcite from Materials Studio package and the Compass forcefield were used to build up a rigid body molecule with *trans* and *gauche* conformations. The intramolecular angles so obtained by this minimization process for both isomers are very close for both conformations, and thus, due to the intriguing disordered structure which prevents a final minimization process of the characteristic intramolecular distances, we average them according to the number of Cl and F atoms (as far as angles are concerned) to get the initial molecular unit in the structure.

By means of a Pawley profile fitting procedure, the cell parameters of an orthorhombic cell were determined, the systematic absences being compatible with the space group *Cmca*. It should be noticed that on cooling from phase I to phase II some Bragg reflections of the OD cubic phase I remain in spite of the annealing (1 h), a result which was already observed in previous works.[37,39]

According to the density requirement, the calculated volume provides $Z = 4$. In general, the *Cmca* space group entails $Z = 16$ with the molecules in general position, so a set of symmetry elements were required in order to decrease such number of molecules. By using the center and a mirror, two molecules (the carbon atoms of which are denoted by C(1b) and C(1c) in Table 4) were placed (see Figure 5, red and blue molecules), both in the *trans* conformation. It should be mentioned here that the *trans* isomer was placed because after a first refinement, the occupancy factor for the Cl and F atoms involved in this molecule gave coherent values (i.e., almost 0 or 1) for these halogens. As it can be seen (Figure 5) Cl atoms are on the mirror while the F atoms

Table 4. Fractional Coordinates of the Intermediate Phase II of ClF_2C-CF_2Cl Obtained at 120 K by Using Neutron Powder Diffraction

atom	*X*	*Y*	*Z*	occupancy
C(1a)	0.1203	0.00000	0.0000	0.75
F(1a)	0.1974	0.0779	0.1115	0.25
F(2a)	0.1974	0.1216	0.0231	0.25
F(3a)	0.1974	0.0437	0.13455	0.25
Cl(1a)	0.2253	0.1023	0.1464	0.125
Cl(2a)	0.2253	0.1597	0.0303	0.125
Cl(3a)	0.2253	0.0574	0.1766	0.125
C(1b)	0.0000	0.0621	0.0480	0.125
F(1b)	0.1706	0.0666	0.1405	0.125
Cl(1b)	0.0000	0.2056	0.0676	0.125
C(1c)	0.0000	0.0119	0.0858	0.125
F(1c)	0.1706	0.0433	0.1525	0.125
Cl(1c)	0.0000	0.1819	0.1307	0.125

are out. In addition, six disordered molecules (denoted as C(1a) in Table 4) were also placed with the C−C bond perpendicular to the (*h*00) plane, i.e., the binary axis due to the molecular symmetry. It then means that the occupancy for the C atoms is 6 times that of the associated Cl atoms. The best fit was obtained with the occupancy factors gathered in Table 4.

The final structure was refined by means of a Rietveld procedure by assuming the described disorder. The structure was confirmed by the reliability factors R_{wp} and R_p reported in Table 2. Figure 6 displays the results of Rietveld refinement for the neutron scattering experiment. It is to be noticed that for this final refinement the characteristic length and angle bonds of the molecules with *trans* conformation (red and blue in Figure 5) were replaced by the original values derived from the molecular energy minimization for such an isomer. For the disordered molecules it was not possible to determine its conformation and additional refinements did not improve noticeably the reliability factors. Nevertheless, according to the results previously published concerning infrared spectroscopy[24,38,39] phase II should keep the same proportion, (48 ± 5)% that the vapor and liquid states. Under such assumption, two molecules with their Cl atoms on the mirror, contributing as one to the unit lattice, are in *trans* conformation, and the four additional disordered molecules over six should be in *gauche* conformation according to the occupancy factors.

3.3. Lattice Symmetry of the High-Temperature OD Phases of Cl_3C-CCl_3 and ClF_2C-CF_2Cl. The orientational disorder of the high temperature phases I of both compounds prevents going beyond a Pawley profile fitting refinement. A model structure containing the short range order was previously published for Cl_3C-CCl_3.[20]

X ray powder diffraction measurements (from 346 to 375 K) of Cl_3C-CCl_3 (Table S3) and the neutron powder diffraction pattern (at 155 K) of ClF_2C-CF_2Cl were indexed according to a body centered cubic lattice which coherently verifies the systematic absences of the *Im*3*m* space group found previously[20,33] for Cl_3C-CCl_3 and related halogen ethane compounds.[13] As for ClF_2C-CF_2Cl the cubic lattice parameter at 155 K was determined to be 6.683 (11) Å. Lattice parameters as a function of temperature for the OD phase of Cl_3C-CCl_3 are reported in Supporting Information and compare well with those previously reported, 7.508 Å at 375 K in this work and 7.51 Å at 378 K according to Atoji et al.[33]

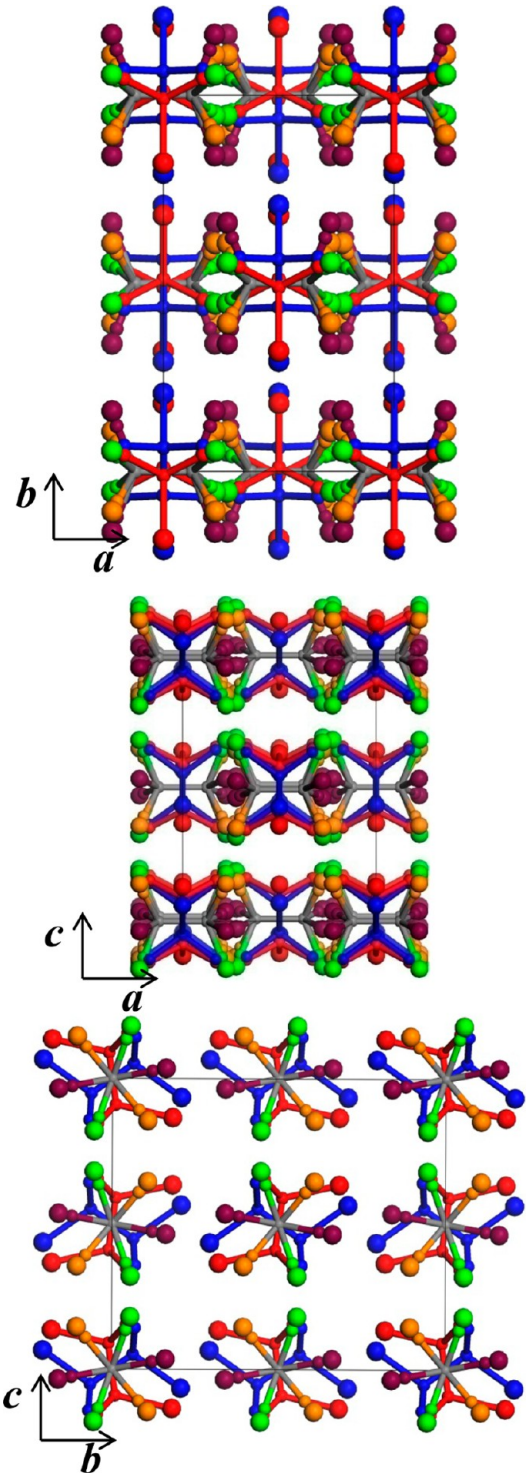

Figure 5. Projection of orthorhombic *Cmca* structure of phase II (at 120 K) of ClF_2C-CF_2Cl in the (00*l*) (top), (0*k*0) (middle), and (*h*00) (bottom) planes.

3.4. Lattice Parameters As a Function of Temperature. In order to determine the volume changes at the phase transitions and the thermal expansion tensor, X ray powder diffraction experiments were performed on heating from 100 K up to 375 K for Cl_3C-CCl_3 thus covering all the solid phases.

Results from neutron experiments match well with those of X ray diffraction (see Figures 7 and 8). Standard least squares fits as a function of temperature were performed for the lattice

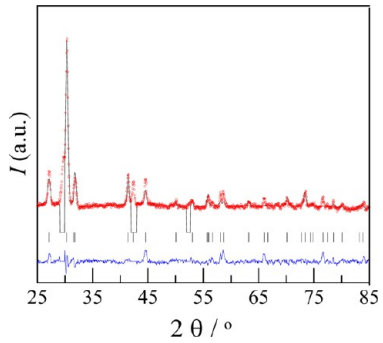

Figure 6. Experimental (red circles) and calculated (black line) neutron diffraction patterns along with the difference profile (blue line) for the final Rietveld refinement of the intermediate phase II of ClF_2C-CF_2Cl at 120 K. Excluded regions for the Rietveld refinement are shown.

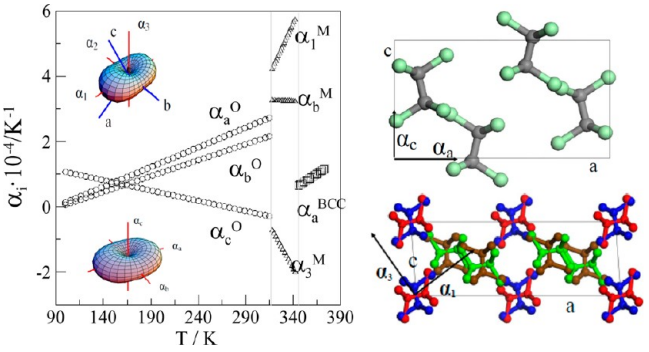

Figure 7. Molar volume for the orthorhombic (diamonds), monoclinic (squares), and body centered cubic (circles) phases of Cl_3C-CCl_3 as a function of temperature from X ray (filled symbols), neutron diffraction (open symbols). Open circles are reported values from Holhweim et al. (at 140 and 294 K),[22] Sasada et al. (at 288 K)[34] and Atoji et al. (at 378 K).[33]

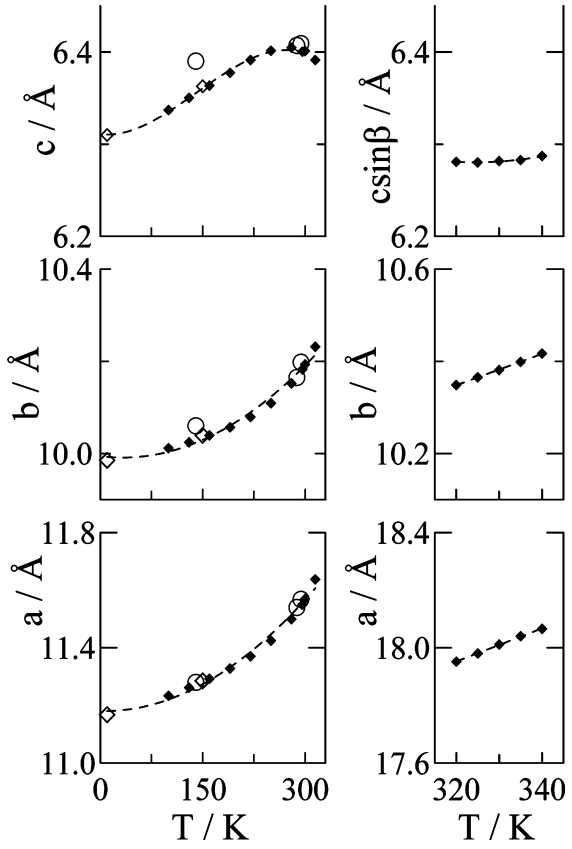

Figure 8. Lattice parameters of Cl_3C-CCl_3 as a function of temperature for phase III (left) and phase II (right) obtained from X ray (filled diamonds) and neutron (open diamonds). Open circles are reported values for phase III from Holhweim et al. (at 140 and 294 K)[22] and Sasada et al. (at 288 K).[34]

parameters and the unit cell volume. Molar volume together with the volume changes at the phase transitions are shown in Figure 7. The polynomials describing the temperature variation for all the phases are gathered in Table 4, while Figure 8 shows the parameters as a function of temperature.

4. DISCUSSION

To examine the intermolecular interactions and the anisotropy, two tools have been used, the thermal expansion tensor and the packing coefficient. The first gives the deformation of the cell dU due to a small temperature variation dT by means of a second rank tensor $dU_{ij} = \alpha_{ij} \cdot dT$, where α_{ij} are the coefficients of the thermal expansion tensor. At a given temperature, knowledge of the principal coefficients and of the direction of the principal axes of the tensor allows the determination of the strongest and the weakest directions of the corresponding intermolecular interactions.[52] Such directions are referred to as "hard" and "soft" directions, respectively.[52,53] The procedure has been published elsewhere and requires the lattice parameter as a function of temperature.[53] According to the Neumann principle, for which the thermal expansion tensor has to display the point group symmetries of the crystal, the tensor corresponding to an orthorhombic lattice is diagonal and the eigenvectors coincide with the axes of the crystal. For a monoclinic lattice, the tensor is defined by the principal coefficients, α_i, i = 1,2,3, and an angle δ between the direction of one of the principal directions and the crystallographic axis a, the α_2 axis being coincident with the 2 fold axis b of the crystal.

Figure 9 (left panel) shows the thermal expansion eigenvalues for the solid phases of C_2Cl_6.

A glance of the eigenvalues for the orthorhombic phase III and the variation with temperature indicates that approaching the III to II phase transition the weakest interactions become even softer on the (00l) plane (soft plane), whereas along the [001] direction strong interactions (hard direction) are present. By comparing the 3D tensors (insets in Figure 9) of phases III and II, and the eigenvalues on the (00l) planes, it can be seen that the (00l) planes in the orthorhombic phase III remain as the soft planes in the monoclinic phase II. Similarly, a direction close to the c crystallographic axis (α_3) is the hard direction in phase II, close to that of phase III. Otherwise, despite the disorder in the monoclinic phase II, the hard (α_3) and soft (00l) planes are very close to those of the orthorhombic phase III. This result is compatible with the proposed mechanism by Woost et al.[21] for the III to II phase transition, according to which high amplitude motions around an axis perpendicular to C−C bond and parallel to the b orthorhombic crystal axis give rise to an increase of the angle between (a, c) in the orthorhombic plane and thus a transformation to a monoclinic structure. It is evident that this transition is first order, so the alleged "*continuity*" of the transition is discarded although the mechanism could be thought of as compatible. A striking feature is the emergence of negative values for the α_3 eigenvalues (contraction) in the monoclinic phase. This experimental result can be due probably to the fact that along such a α_3 direction (see Figure 9 right bottom) a "coexistence" of parallel and perpendicular C−C bonds appears

Table 5. Polynomial Equations $p = p_0 + p_1T + p_2T^2$ (T in K and p in Å or in °) to Which the Lattice Parameters of CCl_3-CCl_3 Were Fitted As a Function of Temperature[a]

phase	temperature range/K	parameter	p_0	$p_1\ 10^3$	$p_2\ 10^5$	$R\ 10^3$
III	100 315	a/Å	11.299(11)	1.27(42)	0.73(10)	0.951
		b/Å	10.067(24)	0.95(25)	0.46(6)	0.323
		c/Å	6.244(17)	1.08(18)	0.19(4)	0.165
II	320 340	a/Å	16.12(3)	5.74(1)		0.008
		b/Å	9.261(18)	3.40(6)	2.4(6)	0.002
		c/Å	8.9(7)	15(4)	54(6)	73
		β/°	45(7)	382(41)		0.068
I	346 375	a/Å	8.2(5)	4(3)	0.7(4)	0.003

[a]The agreement between the calculated and experimental values has been accounted by the reliability factor R, defined as $R^2 = \sum[p_m - p_c]^2/p_c^2)$, where p_m and p_c are the measured and calculated lattice parameters, respectively.

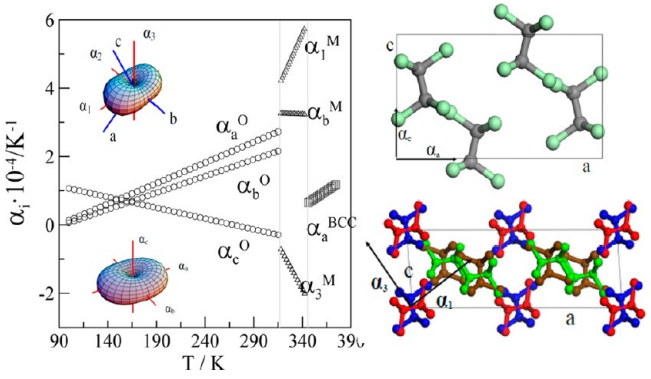

Figure 9. Left panel: The α_i principal coefficients as a function of temperature for Cl_3C-CCl_3: circles, orthorhombic phase III; triangles, monoclinic phase II ($\alpha_2 = \alpha_b$) is chosen parallel to the crystallographic direction b in the monoclinic phase); squares, body centered cubic phase I. The insets are the tensors for orthorhombic phase II at 300 K (bottom) and for monoclinic phase II at 330 K (top) in the frame of the principal directions α_i (red lines) together with the crystallographic axes (blue lines). Right: (0k0) planes for orthorhombic phase III (top) and monoclinic phase II of Cl_3C-CCl_3 with super imposed eigenvectors.

associated with the occupancy factors of the molecules of the unit lattice. The structural similarity between phases III and II concerning the intermolecular interactions suits the small volume (Figure 7) and enthalpy changes for this transition (Table 1).

As it was previously reported, phase III of C_2Cl_6 and phase II of CCl_3-CF_2Cl are isostructural (*Pnma*). In fact, the latter exhibits an occupancy disorder (between one F and the Cl atoms) that enables simulation of the C_{2v} symmetry of the C_2Cl_6 molecule. It can be seen that the eigenvalues here reported for CCl_3-CCl_3 order virtually in the same way that those of CCl_3-CF_2Cl (see Figure 5 in ref 13). Unfortunately we could not afford the measurements as a function of temperature for ClF_2C-CF_2Cl by using neutron scattering. Nevertheless, we can compare the results of this work with other involving fully halogenated ethane derivatives and see how the intermolecular interactions can deform the intramolecular distances. Table 6 gathers some characteristic intramolecular bonds and angles for a set of fully halogenated ethane derivatives. Molecules in the Table 6 are ordered in such a way that the number of F atoms increases (number of Cl decreases) going right. As far as the C−C distances are concerned, we observe that values are ranged between 1.52 and 1.58 Å, clearly above the values found for non perhalogenated compounds. Thus, for 1,1,1 trichloroethane,[54] 1,1,1,2 tetrachloroethane,[9] and 1,1,2,2 tetrachloroethane,[12] C−C distances were reported to be clearly smaller, 1.492 Å, 1.519 Å, and 1.504−1.508 Å, respectively. Even in the high pressure phases for some of these materials, this C−C distance is still below the quoted values for the fully halogenated compounds (1.517 Å for 1,1,1 trichloroethane[54] at 2.15 GPa and for 1,1,1 trichloroethane[54] at 1.65 GPa, or 1.531 Å for 1,1,2,2 tetrachloro ethane at 0.65 GPa).[12]

Table 6. Molecular Bond Lengths (Å) and Angles (°) of the Cl_3C-CCl_3 and ClF_2C-CF_2Cl[a]

molecule	$Cl_3C\ CCl_3$	$Cl_3C\ CCl_3$	$Cl_3C\ CF_2Cl$[b]	$ClF_2C\ CF_2Cl$	$F_3C\ CF_2Cl$[b]
			→*increasing the number of F atoms*		
Phase	Phase III	*Phase II*	*Phase II*	*Phase II*	Phase II
C(1) C(2)	1.584	*1.586*	*1.529*	*1.516 1.517*	1.537
C(1) Cl(i)	1.767 1.771	*1.776*	*1.779 1.780*	*1.773 1.774*	1.771
C(1) F(i)			*1.342*	*1.345*	1.339 1.345
C(2) Cl(i)	1.771 1.779		*1.772*		
C(1) C(2) F(i)			*110.77*	*111.05 111.2*	112.5
C(1) C(2) Cl(i)	109.7 109.8	*110.48*	*112.47*	*111.94 111.9*	111.4 111.5
C(2) C(1) Cl(i)	109.5 109.7		*110.1 110.7*		
Cl(i) C(l) Cl(i)	109.2 109.7	*108.45*	*108.3 108.6*		
F(i) C(1) F(i)				*106.18 107.7*	107.0 107.5
F(i) C(2) F(i)			*106.8*		106.5
F(i) C(2) Cl(i)			*107.9*	*108.20 107.3*	107.8 107.98

[a]For the sake of comparison, values of the low temperature phases of Cl_3C-CF_2Cl (orthorhombic *Pnma*) and CF_3-CF_2Cl (monoclinic $P2_1/n$) recently obtained are enclosed. Italic values concern structures with some kind of disorder. [b]Values from ref 13.

On the contrary, the influence of halogen saturation or the type of halogen (Cl or F) in the molecular structure appears much lower for the C−Cl distance. For the perhalogenated molecules in Table 6, such a distance remains within a narrow domain. The same conclusion can be reached when compared with the aforementioned compounds (1.772, 1.787−1.775, and 1.771−1.780 Å for 1,1,1 trichloroethane,[54] 1,1,1,2 tetrachloro ethane,[9] and 1,1,2,2 tetrachloroethane,[12] respectively). Values in the high pressure phases shorten (the smallest reported value corresponds to 1.739 Å for 1,1,1,2 tetrachloroethane at 2.55 GPa). A similar scenario can be drawn for the C−F bond for the three molecules here reported in Table 6. The landscape for the angle is more heterogeneous, and the only trend that emerges concerns the angles in which the F atoms are involved, which remain almost independent for the different compounds. Trivial evidence is also present: the shorter the C−Cl distance, the higher the value of the C−C−Cl angle.

Intermolecular distances contain information about the short range order, but they are not necessarily representative of the "average structure", which is better described macroscopically by parameters as density or packing coefficient. It is defined as the ratio between the molecular volume (Vm) and the volume occupied by a molecule in the lattice (V/Z). Molecular volumes were calculated using van der Waals radii by the Kitagorodsky's method.[55] Packing values are collected in Table 7. It is worth noting that the packing values of the intermediate phases II of Cl_3C-CCl_3 (0.692 at 323 K) and ClF_2C-CF_2Cl (0.689 at 120 K), despite the high temperature at which they are reported, are relatively small when compared to the other. These experimental facts highlight the significant effect of the disorder in both phases. Such disorder, from a packing point of view, simulates structures similar to those in which different conformations coexist, which is known to have an effect on the average packing.[56,57] For phase II of CCl_3-CF_2Cl, it should be mentioned that the disorder concerns exclusively one F and one Cl atom, so the packing is ranged within the values corresponding to ordered structures.

Table 7. Shortest Intermolecular Distances (in Å)[a]

molecule	Cl_3C CCl_3	Cl_3C CCl_3	CCl_3-CF_2Cl[b]	ClF_2C CF_2Cl	CF_3-CF_2Cl[b]
phase	III (10 K)	II (323 K)	II (5 K)	II (120 K)	II (10 K)
packing	0.768	*0.692*	*0.734*	*0.689*	0.747
			→*increasing the number of F atoms*		
C C C C	6.310	*5.910*	*5.501*	*5.378*	4.980
Cl Cl	3.499	*3.710*	*3.504*	*3.245*	3.766
Cl F			*3.178*	*3.002*	3.319
F F			*3.790*	*2.717*	2.820

[a]C−C···C−C stands for the middle of the C−C bond of the molecule. Italic values concern structures with some kind of disorder. [b]Values from ref 13.

It can be also seen from Table 7 that the efficient packing of phase III of CCl_3-CCl_3 is related to the short Cl···Cl distances because in regard to the center to center molecular distances it reaches the longest value among the examples gathered in Table 7.

5. CONCLUSIONS

The polymorphism of CCl_3-CCl_3 has been reexamined. The previous reported phase transitions have been confirmed and the structure of the long time unknown phase II has been reported. It consists on a monoclinic ($C2/m$) disordered structure with $Z = 6$ molecules. Lattice parameters as a function of temperature enabled us to determine the volume changes at the phase transitions and to verify the thermodynamic coherence with the pressure−temperature phase diagram reported by Knorr.[29] Lattice parameters were also used to get the thermal expansion tensor for the analyzed phases and to conclude that despite the disorder in the monoclinic phase II, the hard (α_3) and soft ($(0k0)$ planes) directions are very close to those of the orthorhombic ordered phase III. These arguments are in favor of the imagined mechanism for the III to II phase transition by Woost et al.[21]

In addition, the room temperature vapor phase of ClF_2C-CF_2Cl was condensed and its polymorphic behavior was studied. The structure of the intermediate phase II was determined to be disordered with orthorhombic ($Cmca$, $Z = 4$) symmetry. By combining the structural results and previous infrared spectros copy studies, it has been concluded that two *trans* and two *gauche* molecules are present. The high temperature OD phase I of this compound was found to be body centered cubic with systematic absences compatible with the OD phase of CCl_3-CCl_3 ($Im3m$).

The occupancy site disorder of the intermediate phases II for both CCl_3-CCl_3 and ClF_2C-CF_2Cl is very close, despite the difference in space groups. Comparison with other perhalo genated derivatives shows that, as for the intramolecular distances, C−C and C−Cl are little dependent on the kind of involved halogens. On the contrary, C−C bond length is much shorter for related halogen ethane derivatives in which H atoms are present.

Finally, it seems that molecular packing is sterically hindered when disorder is present. On that score, packing coefficient of phases II of Cl_3C-CCl_3 and ClF_2C-CF_2Cl in which occupancy site disorder exists is below the most typical values for their counterpart ordered phases (as phase III of Cl_3C-CCl_3).

AUTHOR INFORMATION

Corresponding Author

*E mail: josep.lluis.tamarit@upc.edu.

Notes

The authors declare no competing financial interest.

ACKNOWLEDGMENTS

This work was supported by the Spanish Ministry of Science and Innovation (Grant FIS2011 24439) and the Catalan Govern ment (Grant 2009SGR 1251).

We thank FRM II and ILL for providing beam time on the high resolution powder diffraction beams SPODI and D2b, respectively, and C. Cabrillo for supplying us the experimental setup for in situ gas condensation of ClF_2C-CF_2Cl on the D2B sample holder.

REFERENCES

(1) McCulloch, A. *Environ. Monit. Assess* **1994**, *31*, 167.
(2) Cavallini, A. *Int. J. Refrig.* **1996**, *19*, 485.

(3) Brunelli, M.; Fitch, A. N. *Z. Kristallogr.* **2002**, *217*, 395.
(4) Brunelli, M.; Fitch, A. N. *J. Synchrotron Rad.* **2003**, *10*, 337.
(5) Klug, H. P. *Z. Kristallogr.* **1935**, *90*, 495.
(6) Klug, H. P. *J. Chem. Phys.* **1935**, *3*, 747.
(7) Milberg, M. E.; Lipscomb, W. N. *Acta Crystallogr.* **1951**, *4*, 369.
(8) Boese, R.; Bläser, D.; Haumann, T. *Z. Kristallogr.* **1992**, *198*, 311.
(9) Bujak, M.; Katrusiak, A. *CrystEngComm* **2010**, *12*, 1263.
(10) Bujak, M.; Podsiadlo, M.; Katrusiak, A. *Chem. Commun.* **2008**, *37*, 4439.
(11) Bujak, M.; Budzianowski, A.; Katrusiak, A. *Z. Kristallogr.* **2004**, *219*, 573.
(12) Bujak, M.; Bläser, D.; Katrusiak, A.; Boese, R. *Chem. Commun.* **2011**, *47*, 8769.
(13) Negrier, Ph.; Barrio, M.; Tamarit, J. Ll.; Pardo, L. C.; Mondieig, D. *Cryst. Growth Des.* **2012**, *12* (3), 1513.
(14) Pardo, L. C.; Barrio, M.; Tamarit, J. Ll.; López, D. O.; Salud, J.; Negrier, Ph.; Mondieig, D. *J. Phys. Chem. B* **2001**, *105*, 10326.
(15) Salud, J.; López, D. O.; Barrio, M.; Tamarit, J.Ll.; Oonk, H. A. J.; Haget, Y.; Negrier, Ph. *J. Solid State Chem.* **1997**, *133*, 536.
(16) Jenau, M.; Reuter, J.; Tamarit, J. Ll.; Würflinger, A. *J. Chem. Soc. Faraday Trans.* **1996**, *92*, 1899.
(17) Allen, G.; Brier, P. N.; Lane, G. *Trans. Faraday Soc.* **1967**, *67*, 824.
(18) Mark, J. E.; Sutton, C. *J. Am. Chem. Soc.* **1972**, *94*, 1083.
(19) Vippagunta, S. R.; Brittain, H. G.; Grant, D. J. W. *Adv. Drug. Delivery Rev.* **2001**, *48*, 3.
(20) Gerlach, P.; Hohlwein, D.; Prandl, W.; Schulz, F. W. *Acta Crystallogr.* **1981**, *A37*, 904.
(21) Woost, B.; Bougeard, D. *J. Chem. Phys.* **1986**, *84*, 4810.
(22) Hohlwein, D.; Nägele, W.; Prandl, W. *Acta Crystallogr. B* **1979**, *35*, 2975.
(23) Seki, S.; Momotani, M. *Bull. Chem. Soc. Jpn.* **1950**, *23*, 30.
(24) Yamamoto, S.; Nakasugi, N.; Hamada, A. *J. Korean Phys. Soc.* **1998**, *32*, S857.
(25) Dunning, W. J. *J. Phys. Chem. Solids* **1961**, *18*, 21.
(26) van Braak, J.; López, D. O.; Salud, J.; Tamarit, J.Ll.; Jacobs, M. H. G.; Oonk, H. A. J. *J. Cryst. Growth* **1997**, *180*, 315.
(27) Criado, A.; Muñoz, A. *Mol. Phys.* **1994**, *83*, 815.
(28) Muñoz, A.; Criado, A. *Mol. Phys.* **1995**, *84*, 1207.
(29) Knorr, K. *Z. Kristallogr.* **1983**, *162*, 142.
(30) Gerlach, P.; Prandl, W.; Lefevre. *J. Mol. Phys.* **1983**, *49*, 991.
(31) Mackowiak, M.; Sinayvsky, N.; Bluemich, B. *J. Mol. Struct.* **2005**, *743*, 53.
(32) Watari, F.; Aida, K. *J. Mol. Spectrosc.* **1967**, *24*, 503.
(33) Atoji, M.; Oda, T.; Watanabe, T. S. *Acta Crystallogr.* **1953**, *6*, 868.
(34) Sasada, Y.; Atoji, M. *J. Chem. Phys.* **1953**, *21*, 145.
(35) Mizushima, S.; Morino, Y.; Simanouti, T.; Kuratani, K. *J. Chem. Phys.* **1949**, *17*, 838.
(36) Gerlach, P.; Prandl, W. *Acta Crystallogr.* **1988**, *44*, 128.
(37) Kolesov, V. P.; Kosarukina, E. A.; Zhogin, D.Yu.; Poloznikova, M. E.; Pentin, Yu.A. *J. Chem. Thermodyn.* **1981**, *13*, 115.
(38) Iwasaki, M. *Bull. Chem. Soc. Jpn.* **1958**, *31*, 1071.
(39) Kagarise, R. E. *J. Chem. Phys.* **1957**, *26*, 380.
(40) Stull, D. R. *Ind. Eng. Chem.* **1947**, *39*, 517.
(41) Erastov, P. A.; Kolesov, V. P. *Thermochim. Acta* **1986**, *109*, 175.
(42) Reuter, J.; Büsing, D.; Tamarit, J. Ll.; Würflinger, A. *J. Mater. Chem.* **1997**, *7*, 41.
(43) Hoelzel, M.; Senyshyn, A.; Juenke, N.; Boysen, H.; Schmahl, W.; Fuess, H. *Nucl. Instr. Meth. A* **2012**, *667*, 32.
(44) Hewat, A. W. *Phys. B Cond. Matt.* **2006**, *385−86*, 979.
(45) Ballon, J.; Comparat, V.; Pouxe, J. *Nucl. Instrum. Methods* **1983**, *217*, 213.
(46) Evain, M.; Deniard, P.; Jouanneaux, A.; Brec, R. *J. Appl. Crystallogr.* **1993**, *26*, 563.
(47) Rietveld, H. M. *J. Appl. Crystallogr.* **1969**, *2*, 65.
(48) MS Modeling (Materials Studio) version 5.5: http://www.accelrys.com /mstudio/ms modeling.
(49) Neumann, M. A. *J. Appl. Crystallogr.* **2003**, *36*, 356.
(50) Dollase, W. A. *J. Appl. Crystallogr.* **1986**, *19*, 267.
(51) Toraya, H.; Marumo, F. *Mineral. J.* **1981**, *10*, 211.
(52) Salud, J.; Barrio, M.; López, D. O.; Alcobe, X.; Tamarit, J.Ll. *J. Appl. Crystallogr.* **1998**, *31*, 748.
(53) Weigel, D.; Beguemsi, T.; Garnier, P.; Berar, J. F. *J. Solid State Chem.* **1978**, *23*, 241.
(54) Bujak, M.; Podsiad, M.; Katrusiak, A. *CrystEngComm* **2011**, *13*, 396.
(55) Bond lengths and van der Waals radii were taken from Kitaigorodskii, A. *Organic Chemical Crystallography*; Consultants Bureau: New York, 1961.
(56) Ibberson, R. M.; Telling, M.T. F.; Parsons, S. *Cryst. Growth Des.* **2008**, *8*, 512.
(57) Negrier, Ph.; Barrio, M.; Tamarit, J. Ll.; Veglio, N.; Mondieig, D. *Cryst. Growth Des.* **2010**, *10*, 2793.